Science Advances

AAAS

advances.sciencemag.org/cgi/content/full/3/11/e1603117/DC1

Supplementary Materials for

Ultrafast magnetization reversal by picosecond electrical pulses

Yang Yang, Richard B. Wilson, Jon Gorchon, Charles-Henri Lambert, Sayeef Salahuddin, Jeffrey Bokor

Published 3 November 2017, *Sci. Adv.* **3**, e1603117 (2017)
DOI: 10.1126/sciadv.1603117

This PDF file includes:

- Supplementary Text
- fig. S1. Magnetic properties of the GdFeCo stack.
- fig. S2. Schematic of the experimental setup for measuring the temporal profile of the electrical pulse.
- fig. S3. Temporal current density profiles in CPS.
- fig. S4. Energy spectral density of the electrical pulse, calculated as the square of the Fourier transform of the electrical pulse in the time domain.
- fig. S5. Frequency-dependent absorption calculation on CPS.
- fig. S6. Evolution of the out-of-plane component of the magnetization after arrival of a 9-ps electrical pulse due to SOTs.
- Reference (*43*)

Supplementary Text

Sample Fabrication details

The ~100 nm of MgO is deposited via RF-Sputter onto the sample with an Ar/O_2 ratio of 16 to 1 at a pressure of 4.7 mT and power of 60 W.

We use two layers of photoresist for all the photolithography steps prior to film deposition and lift-off. First, we spin coat a layer of LOR-5A (MicroChem) at 4100 RPM for 30s, followed by a bake at 150 ^{0}C for 10 min. Second, we spin coat the sample with a layer of OiR 906-12 (Dow Chemical) at 4100 RPM for 30 s followed by a soft bake at 90 ^{0}C for 1 min. To pattern the photoresist, we expose the sample to 130mJ cm^{-2} with a Karl Suss MA6 Mask Aligner. Then, the sample is developed with OPD 4262 (Fujifilm) for 40s. Next, either an MgO, Ta/GdFeCo/Pt, or Ti/Au film is deposited. Finally, lift-off off the photo-resist is performed by soaking the sample in Remover PG (MicroChem) over 12 hours.

Influence of spin orbit torques on magnetic dynamics

The spin transfer torque is mediated by conduction electrons and because the conduction in GdFeCo is dominated by the FeCo electrons, we first assume that the torque is acting only on the FeCo sublattice. We set thus $\theta_{FL\_Gd} = \theta_{DL\_Gd} = 0$. Figure S6A shows the change in out-of-plane magnetization when the film is subjected to the current pulse, assuming a spin Hall angle of 0.18, either generating a purely damping-like torque ($\theta_{DL\_Fe} = 0.18, \theta_{FL\_Fe} = 0$) or a field-like torque ($\theta_{FL\_Fe} = 0.18, \theta_{DL\_Fe} = 0$). Zero delay time corresponds to the electrical pulse arrival. No major difference is observed between the two types of torques, and the influence is similar in both cases (~ 8% change in M_z).

Figure S6B shows the influence of the torque assuming the full torque was applied on the Gd sublattice. We obtain a similar change in magnetization as in the previous case where the torque was applied on the FeCo sublattice.

Finally, for fig. S6C we assume that the torque is acting on both sublattices. In this case, the damping like torque is more efficient than the field like torque but overall, the change in magnetization remains smaller than 10%.

Moreover, even if we assumed a scenario were spin orbit torques acted on the effective ferromagnet of total magnetization $M_S = M_{Fe} - M_{Gd}$, switching would be very unlikely as magnetization switching of out-of-plane ferromagnets via spin orbit torques generally requires the use of an external magnetic field (non-existent in our experiments) to break the symmetry of the system (*43*).

Heating of the film via the ultrafast Joule effect will modify the magnetization of the sublattices, as well as the spin orbit torques and magnetization dynamics. However, the study of ultrafast spin injection along with ultrafast heating is a highly challenging problem, on which we will focus in future works.

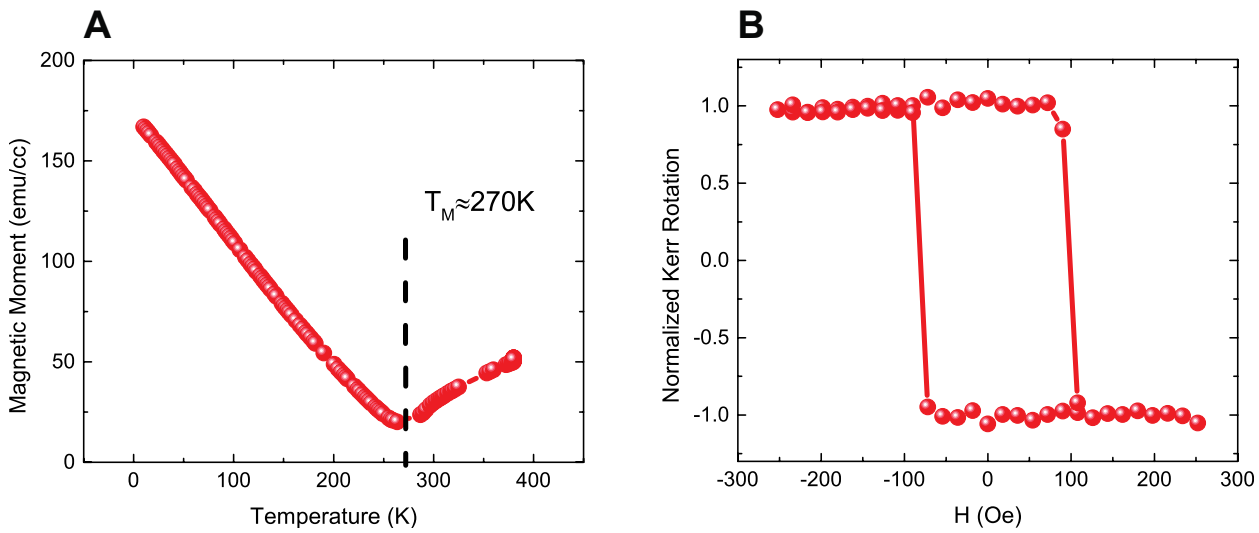

fig. S1. Magnetic properties of the GdFeCo stack. (**A**) Magnetic moment of the GdFeCo film measured with a superconducting quantum interference device (SQUID) at various temperatures. An out-of-plane external magnetic field of 500 Oe is applied during all the measurements. (**B**) Magnetic hysteresis curve of the GdFeCo film at room temperature, measured with the MOKE microscope.

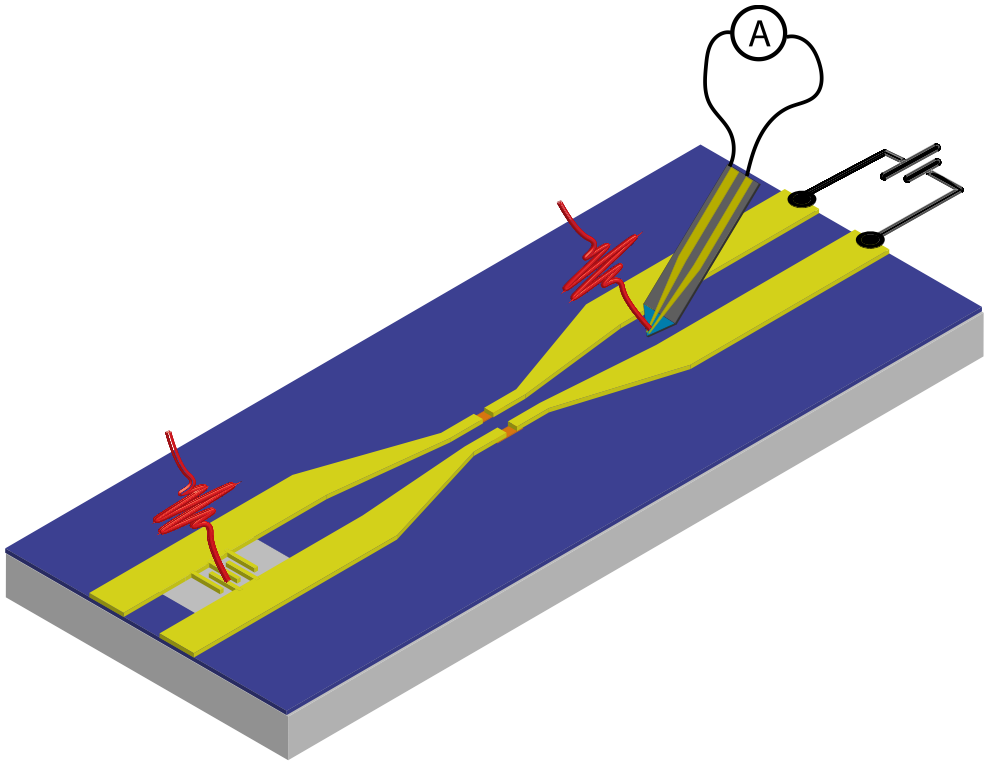

fig. S2. Schematic of the experimental setup for measuring the temporal profile of the electrical pulse. A pump beam is on the photoconductive switch to generate the pulse. A probe beam is on the photoconductive switch at the tip of Protemics Spike probe. A current amplifier is connected to Protemics Spike probe to measure the average current induced by the transient electric field at the tip of the probe. Current profile in fig. S3 is measured before the GdFeCo section as oppose to this schematic.

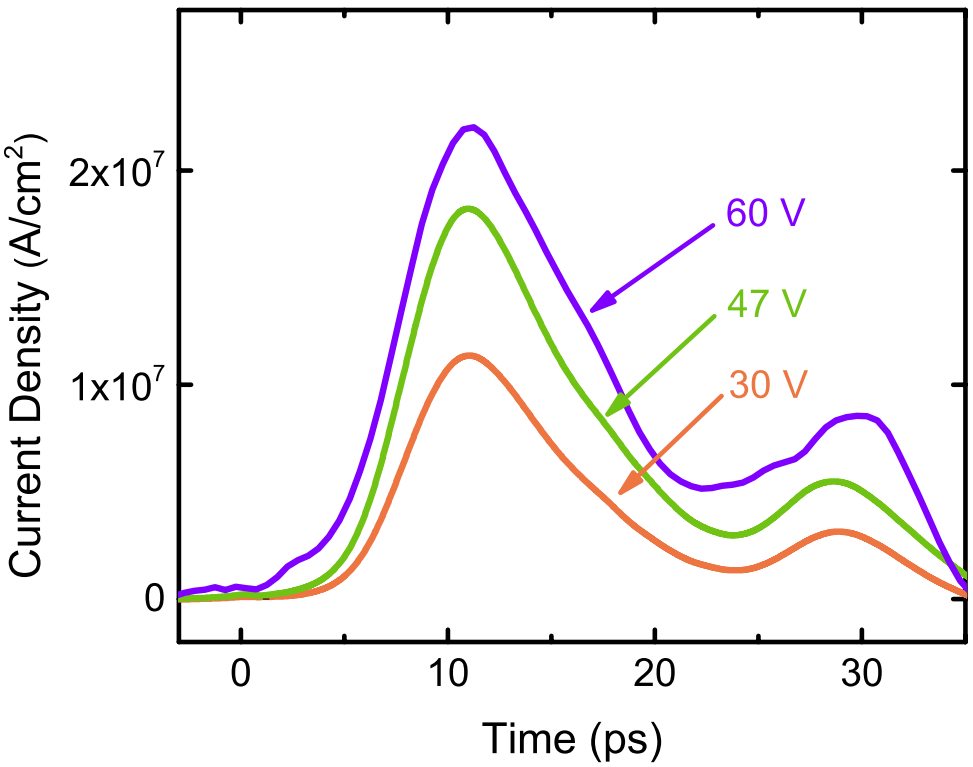

fig. S3. Temporal current density profiles in CPS. Temporal current density profile generated by the photo-switch in 50 μm wide CPS Au line with different biases, as measured with Protemics Spike probe positioned 1mm before the GdFeCo section. The smaller electrical pulse following the main peak is attributed to electrical reflection from the GdFeCo section in the CPS.

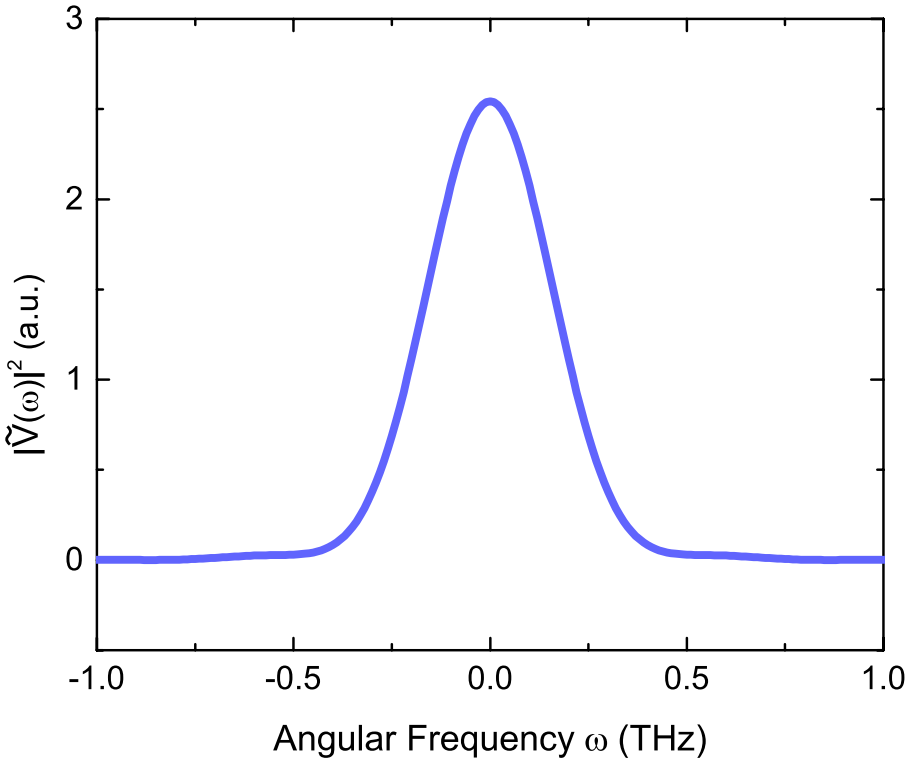

fig. S4. Energy spectral density of the electrical pulse, calculated as the square of the Fourier transform of the electrical pulse in the time domain.

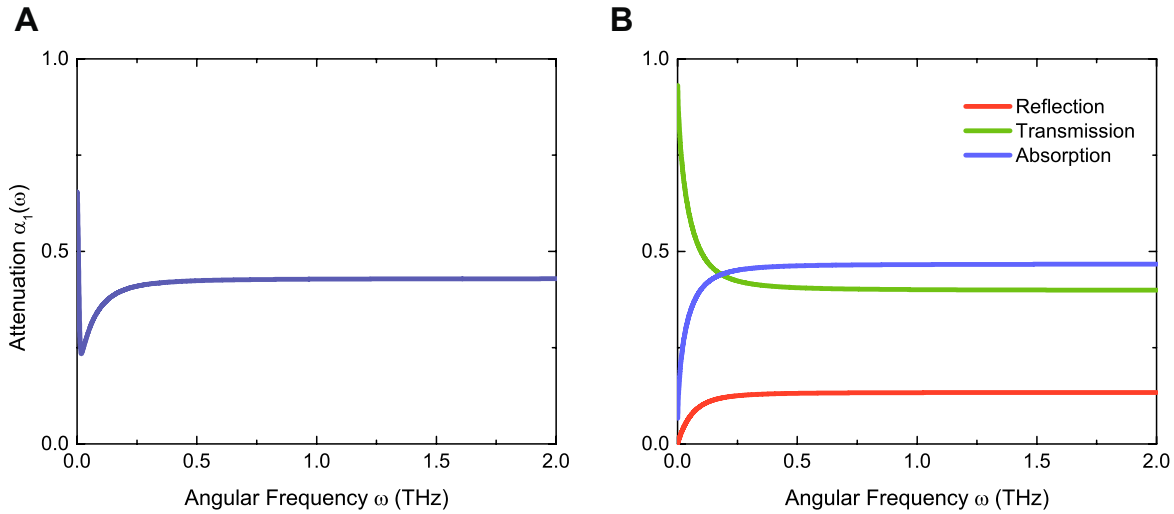

fig. S5. Frequency-dependent absorption calculation on CPS. (**A**) Attenuation of different frequency components on the CPS before the GdFeCo section. (**B**) Reflection, transmission and absorption across the GdFeCo section at various frequencies.

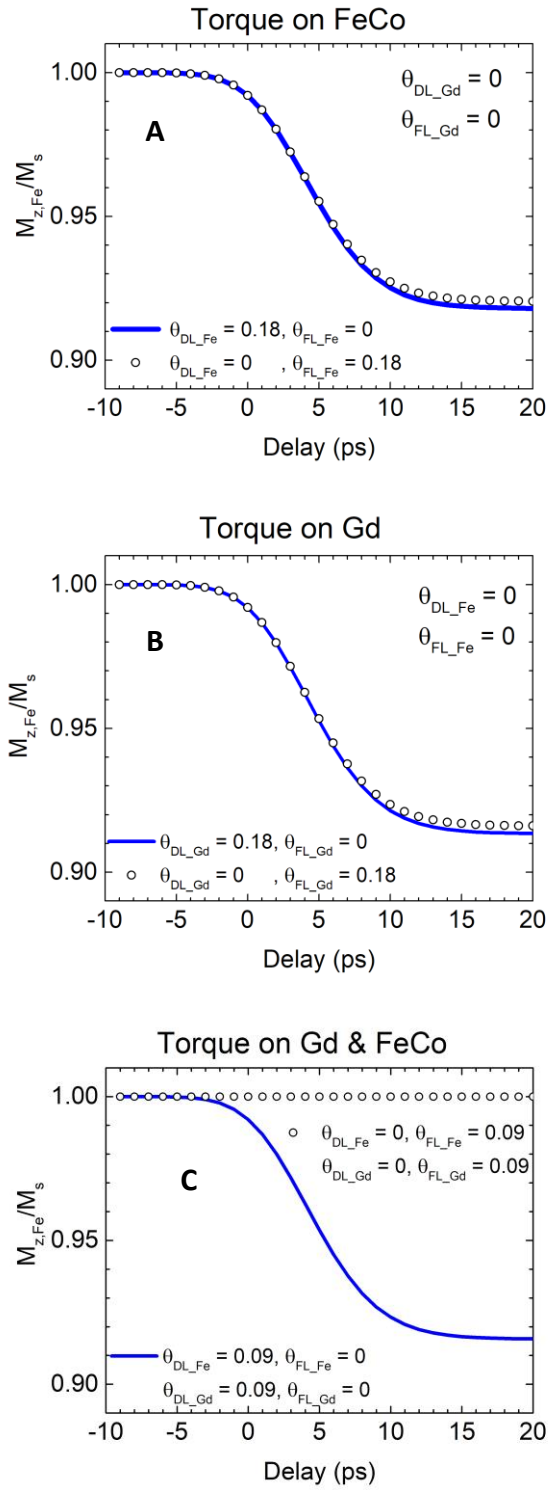

fig. S6. Evolution of the out-of-plane component of the magnetization after arrival of a 9-ps electrical pulse due to SOTs. The torque is applied on the (**A**) FeCo sublattice, (**B**) the Gd sublattice and (**C**) both sublattices simultaneously.